CO_2 Utilization under Intermittent Electricity Supply: Sorption Enhanced DME Synthesis with an Integrated RSOC Process

Jannik Bothe, B.Sc.[a]; Johanna Güttler, B.Sc.[a]; Mathis Heyer, B.Sc.[a]; Dion Jakobs, B.Sc.[a]; Jan Pavšek [a]

[a] *Aachener Verfahrenstechnik, RWTH Aachen University, 52074 Aachen, Germany*

April 2022

Abstract

The restructuring of the chemical industry towards the use of CO_2 and intermittent, renewable energy sources poses a significant challenge for chemical engineers. Based on a systematic screening of current carbon-based chemical processes, we identify a promising combined reversible solid oxide cell (RSOC) and sorption-enhanced DME synthesis (SEDMES) process which produces dimethyl ether from captured CO_2 and wind-generated electricity. Existing flowsheet alternatives are researched and a novel process design is proposed and simulated using Aspen Plus® and MATLAB®. The optimization is divided into a design and a demand side management problem, solved by a genetic algorithm and the linear programming solver CPLEX, to determine the optimal operation and optimal production regime dependent on dynamic renewable electricity availability and price.
The thermodynamic, economic, and ecological performance is assessed and compared to a selected fossil based state-of-the-art and biomass based state-of-research DME process. Thermodynamically, the RSOC/SEDMES process outperforms the exergetic efficiency of the state-of-the-art (37.7 %) and state-of-research (50.8 %) process with an exergetic efficiency of 53.2 %. The necessary product break-even price of 2.14 €/kg_{DME} is approximately five times larger than for the fossil based state-of-the-art process (0.4 €/kg_{DME}), but is more economically viable than the state-of-research process (2.64 €/kg_{DME}). Emitted greenhouse gases calculated via a cradle-to-gate life cycle assessment (LCA) using the GREET® database of $-1.973\,kg_{CO_2eq}/kg_{DME}$ is comparable with the state-of-research process ($-1.813\,kg_{CO_2eq}/kg_{DME}$), and represents a massive improvement over the state-of-the-art process ($2.066\,kg_{CO_2eq}/kg_{DME}$).

1. Introduction

Reducing greenhouse gas emissions to limit global warming to 1.5 °C is the main goal of the Paris Agreement [1]. To achieve this, the entire industrial sector must be transformed toward sustainability, which also poses major challenges in the chemical industry. Currently, chemical processes are primarily based on stationary energy supplies and utilize fossil carbon sources as a feedstock [2]. To enable carbon-neutral chemical production, the next generation of processes must utilize carbon that originate from non-fossil sources. These processes should additionally be able to take advantage of the intermittent energy supplied by the increasing renewable energy production.
Within the scope of this work, several existing processes for carbon-based products are systematically screened, and a novel production route is developed based on the combination of two promising existing processes [3, 4]. During the process development, different design choices are considered in order to enhance the performance and competitiveness. After the process design, a plant optimization is performed. This is followed by a demand side management (DSM) optimization, which determines the best production strategy for reacting to an intermittent renewable energy supply. Finally, a process performance assessment is conducted to compare this novel process with existing state-of-the-art [5] and state-of-research processes [6].

2. Systematic Screening of Chemicals and Process Pathways

The selection of a suitable chemical product and an associated chemical process, which is capable of utilizing captured carbon dioxide and is able to operate under intermittent energy supply, is demanding. Several factors, such as economic viability, ecological impact, and thermodynamic efficiency must be considered and weighed. To determine viable candidates among researched captured carbon utilization (CCU) chemicals, a semi qualitative analysis of economic, ecological and thermodynamic viability is performed in accordance with Chauvy et al. [7]. Seven key performance indicators (KPIs) were selected based on previous research on CO_2 utilization technologies [7–9].
Economic Indicators: *Competitiveness* is the ratio of

the product price when synthesized from captured CO_2 and renewable energy sources as opposed to a traditional fossil based synthesis. *Market Size* is defined as the global amount of the investigated chemical which is produced per year. *Process Complexity* is defined as the relative complexity of used equipment or material required for the process. It is used as a simple estimate for the capital expenditures (CAPEX) of a process.

Ecological Indicators: *Annual Global Warming Potential* (GWP) reduction is defined as the market size weighted reduction in GWP when a product is produced via a green synthesis pathway as opposed to the traditional fossil based pathway [10]. *Renewable Energy Utilization* is defined as the percentage of primary energy a chemical process consumes which can be sourced through renewable energy.

Thermodynamic Indicators: *CO_2 Molar Efficiency* is defined as the amount of CO_2 reactant which is converted into the desired product. *Process Conditions* are defined as an indicator for the maximum temperature and pressure found within a certain process. It is used to generate a simple estimate for the operating expenditures (OPEX) of a process.

The KPIs are compared using a pairwise comparison matrix to determine the normalized weight, and thus importance, of a certain KPI for a chemical product's viability. Figure 1 depicts the pairwise comparison matrix used for this preliminary analysis.

more important than →	Competitiveness	Market Size	Process Complexity	Annual GWP	Utilization of Renewable Energy	Process Conditions	CO_2 Molar Efficiency	Sum	Relative Value	Relative Weight
Competitiveness		1	1	0.5	0	1	1	4.5	4.6	19.3 %
Market Size	0		1	0	0	1	0	2	2.6	10.9 %
Process Complexity	0	0		0	0	0	0	0	1	4.2 %
Annual GWP	0.5	1	1		1	1	0.5	5	5	21.0 %
Utilization of Renewable Energy	1	1	1	0		1	1	5	5	21.0 %
Process Conditions	0	0	1	0	0		0	1	1.8	7.6 %
CO_2 Molar Efficiency	0	1	1	0.5	0	1		3.5	3.8	16.0 %

Figure 1: Pairwise comparison of key performance indicators.

The resulting normalized weights are used in a weighted sum model in which the investigated chemicals and processes are evaluated against one another. The scoring guide for each KPI has been included in the supplementary material. The resulting weighted sum model can be found in Figure 2.

The classes of chemicals investigated are selected from existing research on CCU products [7, 10] and are shown in Figure 2. Synthesis gas (Syngas) consists of H_2, CO and often also CO_2, where the ratios of H_2:CO:CO_2 depend on the further utilization of syngas, as syngas is frequently used as a reactant for other chemical products [4]. In the group of carboxylic acids, the commodity chemical formic acid is primarily considered, which is used for silage preservation [10]. Methanol is used in many reactions and is one of the most important bulk chemicals produced [10]. The organic carbonates considered in the screening are dimethyl carbonates and polyols, which are used to produce plastics [10]. Chemicals primarily designated as fuels can often also be used as bulk chemicals, e.g. methane in dry methane reforming (DMR) to produce syngas or dimethyl ether (DME) to produce aromatics and olefins [11, 12].

From the weighted sum model depicted in Figure 2, the chemicals and associated processes with the highest score are further investigated. The best-rated products are syngas produced by DMR or co-electrolysis and methanol produced via direct hydrogenation of CO_2 (cf. Figure 2). However, the DMR process can only barely use renewable energy and requires CH_4 as the C-source, which either originates from fossil sources or must be produced from CO_2 in an additional step. In contrast, co-electrolysis uses CO_2 and H_2O as reactants under the consumption of electricity, which can be produced via renewable energy [13]. Therefore, co-electrolysis is better suited than DMR in order to utilize CO_2 and renewable energy to produce syngas. Moreover, syngas is used as a reactant for several other screened processes, and can thus be used as an intermediate product for a larger aggregated process. The best-rated processes with a score of 2.9 to 3.1 which utilize syngas are the DME synthesis processes.

The conventional production process of DME is the indirect synthesis via methanol from syngas. The methanol synthesis as well as its subsequent dehydration to DME are thermodynamically limited, resulting in low single pass yields. The combination of both steps in the direct production route results in higher DME yields due to the instantaneous follow-up reaction of methanol to DME, shifting the equilibrium to the product side. Moreover, less process steps are required. However, DME yield is still low and large recycle streams of syngas, CO_2 and methanol are required [4]. Furthermore, the formation of large quantities of H_2O leads to catalytic deactivation [14] and using CO_2 as reactant is not viable due to low CO_2 conversion and DME yield [4].

To overcome this, in situ separation is used to remove the by product H_2O and thus shift the chemical equilibrium to the product side according to Le Chatelier's principle. In addition, thermodynamic limitations are circumvented, and catalyst deactivation is prevented [14].

Two main concepts for the in situ separation of H_2O during DME synthesis have been reported in literature [30]. H_2O can either be separated using a H_2O selective membrane in the reactor [31] or it can be removed from the reacting phase via adsorption (SEDMES). Membranes have the advantage of continuous operation mode instead of

		Rel. weight	H_2/CO - rWGS [15]	H_2/CO - DMR [16]	H_2/CO - Co-electrolysis [17]	HCOOH - Hydrogenation [18]	HCOOH - Hydrogenation [19]	HCOOH - rWGS + Carbonylation [10]	CH_3OH - Direct hydrogen. of CO_2 [20]	CH_3OH - rWGS + hydrogen. of CO [21]	CH_3OH - Co-electrolysis + hydrogen. of CO [22]	CH_3OH - Thermochem. dis. + hydrogen. of CO [23]	DMC - Transesterification of urea [24]	DMC - Electrochemical production [25]	Polyol - PO/CO_2 copolymerization [26]	CH_4 - Sabatier [27]	Diesel - Fischer-Tropsch [28]	Jet Fuel - Fischer-Tropsch [28]	DME - Direct synthesis [29]	DME - SEDMES [4]	DME - Co-electrolysis + SEDMES
			Synthesis Gas			Carboxylic Acids			Methanol				Organic Carbonates			Fuels and Oxygenates					
Economic Factors	Competitiveness	19.3 %	3	4	1	4	4	1	4	4	4	4	5	1	5	2	4	4	4	4	4
	Market Size	10.9 %	5	5	5	1	1	1	2	2	2	2	1	1	2	3	3	3	2	2	2
	Process Complexity	4.2 %	3	2	4	3	3	4	3	2	2	3	2	4	2	3	2	2	2	1	1
Ecological Factors	Annual GWP	21.0 %	5	5	5	2	2	2	3	3	3	3	1	1	1	3	3	3	3	4	4
	Utilization of Renewable Energy	21.0 %	1	1	5	3	3	2	5	1	5	3	1	3	1	1	1	1	1	1	5
Thermodynamic Factors	Process Conditions	7.6 %	3	3	3	3	2	3	2	2	1	2	2	4	3	3	3	3	2	3	3
	CO_2 Molar Efficiency	16.0 %	5	5	3	4	4	4	5	2	2	2	2	1	5	4	4	4	5	5	5
			3.5	3.7	3.7	2.3	2.2	1.7	3.7	2.4	3.2	2.8	2.0	1.8	2.7	2.5	2.9	2.9	2.9	3.1	3.9

Figure 2: Weighted sum model in which the considered processes are evaluated.

cyclic ad- and desorption. Nevertheless, for separation via membrane, a minimum partial pressure gradient of H_2O of about 1 bar is needed. The synthesis reaction operated under adsorption, instead, does not require for pressures as high as for separation of H_2O over a membrane. Due to side product removal increased pressures are neither required for shifting the equilibrium according to Le Chatelier is necessary. Therefore, SEDMES makes full advantage of lower pressures being possible during DME synthesis. Also, adsorption leads to a higher single pass conversion and DME yield and is therefore the preferred option regarding DME synthesis [30] and consequently considered in the process screening (Figure 2).
The combination of the co-electrolysis (CO_2 and H_2O to syngas) and the SEDMES process (syngas to DME) represents a further process which is also evaluated in Figure 2. Since the combined process merges the advantages of both processes, a score of 3.9 is achieved, resulting in the best rating during the systematic screening. Therefore, this combined process is chosen for the further course of this work.

2.1. Research Gap

In the following, we show that existing research in the field of CO_2 utilization provides a strong basis towards developing a novel process that couples co-electrolysis and DME production. Botta et al. performed a thermodynamic analysis on a process that uses a solid oxide electrolysis cell (SOEC) to produce syngas for a direct DME reactor [32]. Pozzo et al. designed a process where biomass is gasified to a CO_2-rich syngas which is further enriched with CO and H_2 produced in a SOEC. This syngas is then similarly converted to DME via direct DME synthesis [33]. In literature, only one process developed by Skorikova et al. exists where a SEDMES process has been combined with any form of electrolysis [34]. As such, the combination of a co-electrolysis process with a SEDMES process represents a novel production route for DME from captured CO_2.
Modern chemical processes have not been developed to account for intermittent energy sources, which presents a major challenge for the chemical industry when employing many forms of renewable energy. To overcome this challenge, a reversible solid oxide cell (RSOC) is chosen. This type of electrochemical cell can operate in one of two modes, either as an electrolysis cell (EC) which converts electrical energy into chemical energy or as a fuel cell (FC) which performs the reverse reaction [35].
RSOC cells are often used for power-to-X-to-power applications in order to store energy and in most cases H_2 is either produced or consumed [36]. Similar to SOECs that produce syngas, RSOCs are also capable of using a mixture of CO_2 and H_2O as reactants. Er-rbib et al. conducted a performance assessment on an RSOC coupled with a methanation unit, and Wang et al. performed a thermodynamic comparison of different energy storage systems, which also considered a RSOC operated with syngas [3, 37]. Currently, however, there exists no research towards the implementation of an RSOC to produce intermediate syngas for a combined DME production process. Based upon the strong evaluation of the combined co-electrolysis and SEDMES process in the systematic screening with a score of 3.9 and the potential of reversible operation as an answer to challenges derived from intermittent energy sources, a novel combined RSOC and SEDMES process is proposed in this work to produce DME as a bulk chemical for the chemical industry. DME can be used as chemical intermediate for the production of bulk chemicals such as diethyl sulfate, methyl acetate, light olefins and synthetic gasoline [12]. Currently, DME is mainly used as a propellant and coolant [38], and increasingly as an alternative and sustainable fuel for liquid petroleum gas (LPG) and diesel, as well as for power generation in gas turbine plants [12]. A huge advantage of DME is that it is neither toxic nor carcinogenic, and is also not ozone-depleting [14].

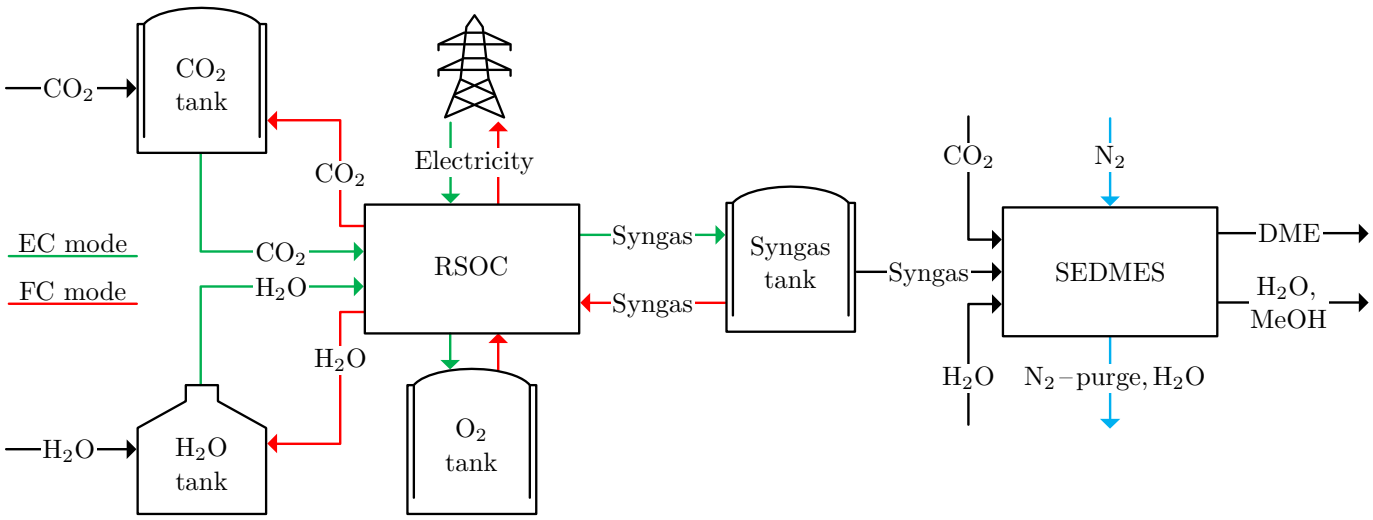

Figure 3: Overall process deisgn

3. Process Design and Simulation

In the following sections, the overall design of the combined process and the individual sub-processes are introduced. Process design choices are elaborated upon and an overview of the process modeling and simulation is given.

3.1. Overall Process Design

The key requirements of the designed RSOC/SEDMES process are to integrate captured CO_2 as a replacement for standard fossil based carbon sources and to use renewable energy sources, which are often intermittent by nature. By storing syngas as an intermediate product and exploiting the reversible nature of the RSOC, the developed process is designed to fulfill both requirements. Figure 3 depicts an overview of the combined RSOC/SEDMES process.
In times of abundant renewable energy, the RSOC can run in EC mode. While in this mode, CO_2 and H_2O react to form syngas using electricity (cf. green paths in Figure 3). This syngas is stored as an intermediate product in a dedicated tank, enabling a constant mass flow to the subsequent steady state SEDMES process. In times of low renewable energy production, the RSOC can be switched to FC mode. Thereby, syngas is provided by the syngas tank and fed to both the SEDMES process and the fuel cell. Within the fuel cell, syngas reacts back to CO_2 and H_2O under the generation of electricity (cf. red paths in Figure 3). This electric energy can either be used to run the balance of plant (BOP) components, especially for the SEDMES process which consumes energy continuously, or it can be fed to the electricity grid for the purposes of grid balancing.
The SEDMES process utilizes temperature pressure swing adsorption to enhance the reaction of syngas to DME. Adsorbent beds capture H_2O produced as a by-product to promote the equilibrium reaction of CO_2 to DME and an additional nitrogen stream is used to regenerate the adsorbent beds (cf. Section 3.3) [4]. Additional CO_2 is fed to the SEDMES process, making use of preferable equilibrium conditions [4].

3.2. CO_2 to Syngas: Reversible Solid Oxide Cell

A reversible solid oxide cell is used for syngas production from CO_2 and H_2O. The following sections outline the process design, important design choices, as well as our approach to modeling the reversible solid oxide cell.

3.2.1. RSOC: Process Description

In the EC mode, CO_2 and H_2O are converted to syngas via the use of electricity. The externally purchased CO_2 is stored and fed at 298 K and 60 bar. After throttling the CO_2 to the cell operating pressure of 5 bar, the CO_2 is mixed with H_2O and is superheated to the cell operating temperature of 1070 K using electric heaters and integrated heat streams. The superheated stream is fed into a solid oxide cell, where the electrolysis of H_2O to H_2 and the (reverse) water gas shift reaction (rWGS, Equation 1) take place simultaneously.

$$CO_2 + H_2 \underset{\text{WGS}}{\overset{\text{rWGS}}{\rightleftharpoons}} CO + H_2O, \ \Delta H^0 = 41\,\text{kJ/mol} \qquad (1)$$

Although the electrolysis of CO_2 to CO is possible, most of the CO_2 reacts with H_2 in the rWGS reaction [13]. This is due to the higher reaction rate of the rWGS reaction compared to that of CO_2 electrolysis and the larger overpotential of the CO_2 electrolysis compared to the H_2O electrolysis [39, 40].
During the water reduction reaction at the cathode, O^{2-}-ions migrate through the electrolyte and oxidize to O_2 at the anode. From there, the produced O_2 is washed out of the cell with pure oxygen. The oxygen by-product is

stored at 298 K and 200 bar, and is partially sold. Yttria-stabilized Zirconia (YSZ) is chosen as an electrolyte due to its high ionic conductivity for O^{2-}-ions at elevated temperatures [41]. To promote the high ionic conductivity of the electrolyte, the operating temperature of the cell should be chosen between 970 K and 1170 K [36, 39]. Moreover, the elevated temperature favors high conversions of CO_2 and H_2 in the rWGS reaction [42].
The cell outflow stream containing CO, H_2, CO_2 and H_2O is cooled and flashed at ambient conditions. The liquid phase, mostly water, is routed to the water storage tank, whereas the gas phase is compressed to 60 bar and stored in the syngas tank at 298 K. The SEDMES process is supplied from this tank continuously.
In the FC mode, the RSOC operates as a fuel cell. Syngas is converted to CO_2 and H_2O, while electricity is generated. Syngas is taken from the syngas tank, expanded and heated to cell conditions 1 bar, 1173 K. Oxygen is provided from the O_2 tank or is bought. The cell outflow containing CO_2, H_2O, CO, and H_2 is routed to an afterburner, where O_2 is used to combust the remaining CO and H_2. The generated heat is integrated with the heat sinks of the process. CO_2 and H_2O are flashed at ambient conditions and fed to their respective tanks.
The flowsheet of the RSOC process is included in the supplementary materials.

3.2.2. RSOC: Design Choices

Prior to the rigorous operating point optimization (subsection 5.1), some superstructure decisions are made. More precisely, three design choices are evaluated based on a preliminary operating point (56 mol/s syngas) reported by Er-rbib et al. [37].
First, a closed oxygen cycle for the air-side of the cell is chosen over the traditional use of ambient air as sweep stream [35, 37, 43–45]. When pure O_2 is used instead of ambient air, the same amount of O_2 can be provided to the cell with a 79 % smaller flow rate. Our calculations show that the hereby reduced compression and heating costs compensate for new costs incurred for storing the oxygen. Furthermore, the O_2-producing EC mode is expected to run longer than the FC mode, so that excess O_2 can be used in the afterburner or sold. Compared to the use of ambient air, the closed cycle design for the selected operating point leads to additional costs of 2.89 €/(h mol_{syngas}) in FC mode, but savings of 11.70 €/(h mol_{syngas}) in EC mode. With the conservative assumption of a balanced EC-FC operating time ratio, the additional equipment required (2 additional compressors, 3 heat exchangers for intercooling, and 1 tank) is amortized after 0.3 years of operation.
Second, the use of a turboexpander in the hot cell outflow stream is investigated as suggested by Redissi et al. [43]. It is found that at moderate operating pressures, using the stream's energy for heat integration is more cost-effective than generating additional electricity with a turboexpander. Only at elevated cell operating pressures, could the turboexpander be economically advantageous. For example, at 15 bar an additional profit of 0.39 €/(h mol_{syngas}) could be generated in the FC mode, taking into account operating costs and capital costs after heat integration. However, we avoid these high operating pressures to prevent the formation of methane in the cell [37].
Third, we decide to use an afterburner to remove remaining CO and H_2 from the FC product stream. Note that the FC product flow is stored and serves as reactant to the EC mode. Accordingly, removing the remaining syngas or converting it into CO_2 and H_2O increases the cell's efficiency in EC mode and reduces the specific volume of the stream to be stored. The afterburner is a simple option here that can also be integrated with the oxygen produced and provides an additional heat source that can be 100 % integrated with the heating of the cell inlet. Absorptive separation of CO_2 from the syngas using the Rectisol process [37] has not proven to be economically viable due to the considerable additional equipment required and the contamination of the stream with methanol.

3.2.3. RSOC: Modeling and Simulation

The RSOC process is modeled in Aspen Plus®. Here, the PSRK model (Predictive Soave Redlich Kwong) is chosen, because it is well suited for polar and non-polar components at high temperatures and pressures [46]. However, Aspen Plus® does not provide any electrochemical blocks. Therefore, a substitute model for the RSOC based on Hauck et al. is used, which consists of two RGIBBS reactors for the rWGS/WGS reaction and one RSTOIC reactor for the electrochemical reaction of water [39].
A MATLAB® [47] script is developed that utilizes the Aspen Plus®-MATLAB® interface [48] to set the simulation parameters such as temperature and pressure for each unit operation block in Aspen Plus®, thus enabling the selection and independent simulation of either the EC or FC mode. Further, this script calculates the reaction rate, cell potential and electrical power consumption of the RSOC using a 0-D model. The electrochemical conversion of CO_2 to CO and vice versa are neglected, and only the reduction and oxidation respectively of H_2O and H_2 are accounted for in the electrochemical reaction calculations. Faraday's law is used to calculate the current during the electrochemical reactions. It is defined in Equation 2 as

$$I = \dot{n}_i \cdot z \cdot F \tag{2}$$

with current I, molar extent of reaction $\dot{n}_i$ of species i, number of transferred electrons per reaction z and Faraday constant F [49]. All electrochemical reactions consist of an oxidation reaction which occurs at the anode and a reduction reaction which occurs at the cathode. However, when changing the RSOC from EC to FC mode, the compartments will change in which the oxidation and reduction

reactions take place. Hence, in further context, the compartment in which H_2O is converted to H_2 and vice versa is named the "fuel side", whereas the other compartment of the cell is called the "air side". At the electrode of the fuel side, Reaction 3 occurs [50].

$$H_2O(g) + 2\,e^- \underset{FC}{\overset{EC}{\rightleftharpoons}} H_2(g) + O^{2-} \tag{3}$$

The O^{2-}-ions needed for this reaction are either produced or consumed at the electrode on the air side. Here, the Reaction 4 takes place [50].

$$O^{2-} \underset{FC}{\overset{EC}{\rightleftharpoons}} \frac{1}{2}\,O_2(g) + 2\,e^- \tag{4}$$

For this electrochemical system, the number of transferred electrons per reaction z is 2. With a given molar extent of reaction n_{H_2}, the current I consumed or produced can be calculated.
To calculate the electric power consumption or production, the cell potential U_{cell} is needed. U_{cell} is defined in Equation 5 as

$$U_{cell} = U_{Nernst} - ASR \cdot \frac{I}{A} \tag{5}$$

with the Nernst potential U_{Nernst}, the area specific resistance ASR and the electrochemical active surface area of the electrode A [37, 39]. The ASR combines several resistances which occur in a cell as a result of activation, ohmic, and concentration losses. By multiplying I and U_{cell}, the electric power P_{cell} can be obtained. The flowsheet of the RSOC process is included in the supplementary materials.

3.3. Syngas to DME: Sorption-enhanced DME Synthesis

A Sorption-enhanced DME Synthesis process is used to convert the syngas produced by the RSOC into the promising platform chemical and fuel DME [34]. The required purity for DME as a bulk chemical is not well specified and may strongly depend on the process in which it is used for. Typical minimum purities for DME that are sold as a chemical vary between 99.8 % and 99.9 % [51]. For the purpose of a fuel, the ISO 16861 defines a minimum mass fraction for DME of 99.5 % before adding any additives [52]. For comparability, this has therefore been selected as target composition for the following process design. In the following sections, the process design, important design choices, as well as the modeling and simulation of this SEDMES process are outlined.

3.3.1. SEDMES: Process Description

The syngas feed and additional CO_2 are mixed with recycled syngas and subsequently fed into the reactor block. The reactor design is adapted from van Kampen et al. [4]. As the saturated adsorbent must be regenerated periodically, at least two reactors are necessary. However, as adsorption is typically faster than desorption, three reactors operated in parallel are sufficient to assure a continuous DME production. At any time, one reactor is producing DME and is adsorbing water, whilst within the other two reactors, water is being desorbed [4]. Based on the research of Van Kampen et al., a temperature pressure swing adsorption reactor system is selected and implemented due to the higher working capacity, compared to individual pressure or temperature swing [4]. In the actively adsorbing reactor column, DME is produced at 548.15 K and 30 bar. In the other non reacting reactors, water is simultaneously desorbed at 673.15 K and 3 bar with nitrogen as purge gas. The advantage of nitrogen as purge gas lies in its inert nature, allowing for an increased regeneration of the adsorbent compared to alternative gases, such as syngas [4]. The nitrogen purge gas stream loaded with desorbed water is then cooled to 320 K. The resulting two phase stream is fed to a flash unit, where the liquid water phase is separated and later used as absorbent in the distillation train.
The DME product stream leaving the reactor block is fed to the distillation train. Firstly, a membrane is used to separate off a fair amount of CO_2 from the product mixture. This is done by using a composite polymer membrane [53] at operating conditions of 548.15 K and 29 bar. With only a small amount of CO_2 remaining in the stream, methanol can be subsequently separated from the stream using a flash. The flash conditions are set to 310 K and 29 bar. In the light product of the flash remains the majority of the DME, CO, H_2 and the rest of the CO_2.
Next, DME is separated from CO, H_2 and residual CO_2 in the flash top stream. Skorikova et al. [34] proposed an overall process design for a sorption enhanced DME synthesis process in which cryogenic conditions are involved in the distillation train. This requires large amounts of energy to prepare the necessary subcooled refrigerant. However, to limit unnecessary energy usages in compliance with Green Chemistry principles, the cryogenic distillation is not utilized in the SEDMES process. An alternative to realize the difficult separation of CO_2 and DME in the presence of traces of MeOH [54] has been proposed by Azizi et al. [38]. They implemented a distillation train using water as absorbent, allowing for cryogenic conditions to be avoided during separation. However, in the liquid product stream of the absorption column, there is still a considerable amount of CO_2 present, which makes it hard to achieve the target composition of 99.5 wt% in the downstream distillation column. Therefore, a stripper is used for the absorption of DME in water, instead of a simple absorption column, as proposed by Azizi et al. [38]. Thereby, the remaining CO_2 is driven out of the liquid stream. This allows for a high recovery of CO, CO_2 and H_2 for recycling back to the reactor. The incorporation of the aforementioned stripper also drives a small amount of DME to the top product of the absorption column and

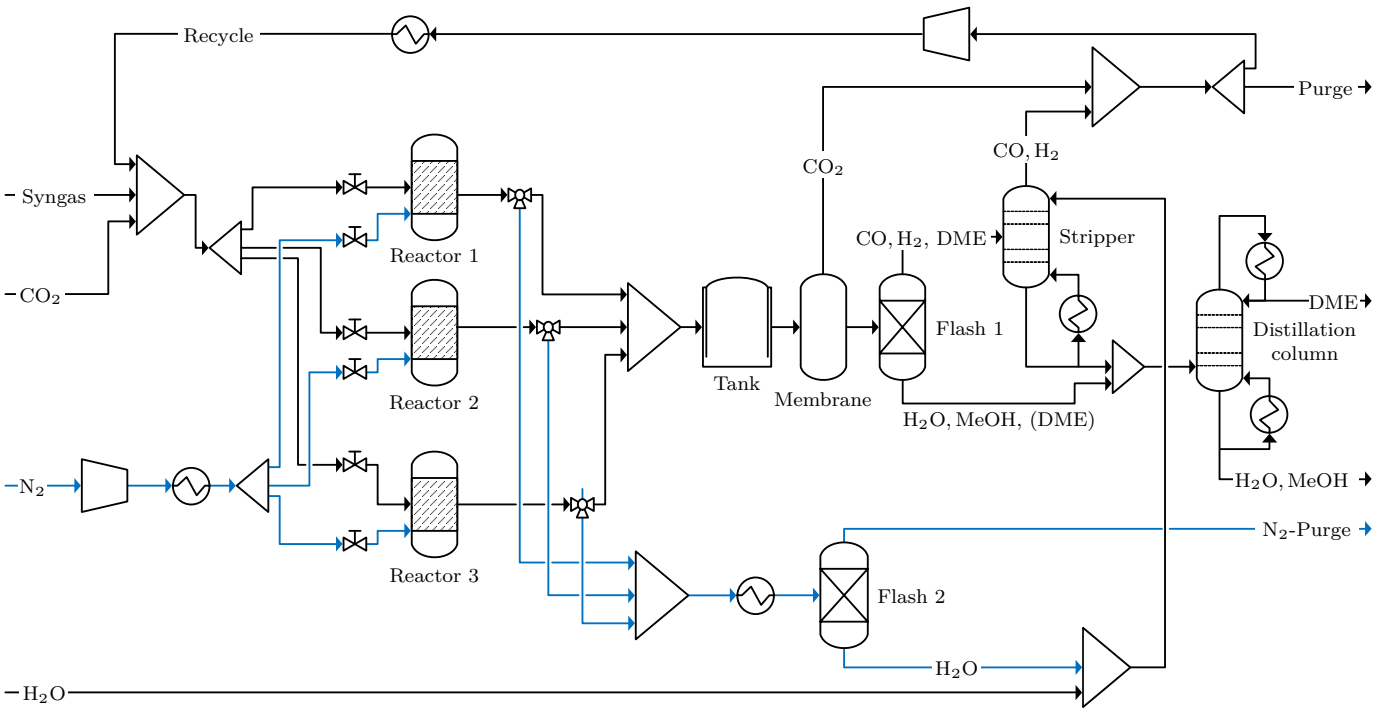

Figure 4: SEDMES Flowsheet

thereby to the recycling stream. However, as the reactor incorporates an enhancement technique, feeding a small amount of product back to the reactor is not expected to impact the conversion negatively. The liquid stream leaving the stripper is subsequently mixed with the liquid stream from the prior flash unit. This is done to recuperate the non trivial amount of DME previously flashed with the MeOH and water. As CO_2 has been separated before, the mixture of DME, methanol and water can now be easily separated using a simple distillation column, with DME as the distillate product. Using a nine stage distillation column with a reflux ratio of 5.14, a constant mass flow of 2365.76 kg/h with a purity of 99.9 % of DME is supplied.The flowsheet of the SEDMES process is included in the supplementary materials.

3.3.2. SEDMES: Design Choices

Besides the choice of the distillation train described in Section 3.3.1, the source of nitrogen was also considered as a further design choice. Nitrogen can either be recycled or fresh nitrogen can be bought. For a recycle of N_2, an additional compressor would be necessary in order to increase the purge stream of nitrogen in pressure back to reactor conditions. In order to evaluate the two design alternatives, the CAPEX of an additional compressor have been calculated using a shortcut method from Guthrie et al. [55]. These calculations result in an estimated capital cost for an additional compressor of 1 493 000 $ Assuming a nitrogen price of 0.92 $/m^3 [56] the operating cost for providing the entire nitrogen stream with fresh N_2 lies at 591 258 $ over the entire lifetime of the plant. Thus, just the capital costs for the compressor already exceeds the costs for the amount of (new) nitrogen needed without recycle. Therefore, a recycle of N_2 is not incorporated.

3.3.3. SEDMES: Modeling and Simulation

Aspen Plus® is used to simulate the SEDMES process. To model a continuous DME production in Aspen Plus®, we implement an RSTOIC reactor representing the three-column system, using reaction conversions reported in literature [30]. To account for the influence of process conditions on the required amount of adsorbent in the reactor and therefore on the size of the reactors, we implemented a shortcut model in MATLAB®. The reactor conditions during water desorption and the molar flow rates of nitrogen, desorbed water, and reactants are fed to the model as inputs. The mass of adsorbent and the reactor volume are generated as outputs. The shortcut model is based on an intracrystalline mass balance (7) which describes the intracrystalline transport of water and the ad- and desorption of the adsorbent:

$$\frac{d\overline{q}}{dt} = k_{LDF,2}(q^{\star} - \overline{q}) \tag{6}$$

$$\Rightarrow \int_{q_{ads,start}}^{q_{ads,end}} \frac{1}{q^{\star}_{ads} - \overline{q}} d\overline{q} = \int_{0}^{t_{ads}} k_{LDF,2} dt \tag{7}$$

$$\Rightarrow \int_{q_{des,start}}^{q_{des,end}} \frac{1}{q^{\star}_{des} - \overline{q}} d\overline{q} = \int_{0}^{t_{des}} k_{LDF,2} dt \tag{8}$$

where $k_{LDF,2}$ is the mass transfer coefficient (Linear driving force rate constant), $\overline{q}$ is the current average adsorbent loading, $q^{\star}$ is the equilibrium adsorbent loading at certain T and p, and $q_{ads,start}$ and $q_{ads,end}$ describe the adsorbent loading at the beginning and at the end of the adsorption, respectively. $q_{des,start}$ is the adsorbent loading at the beginning of the desorption and $q_{des,end}$ is the adsorbent loading at the end of the desorption. Assuming, that no adsorbed water builds up over time, it can be defined that $q_{des,start} = q_{ads,end}$ and $q_{des,end} = q_{ads,start}$. Furthermore, it is assumed that the partial pressure of water remains constant over the length of the reactor, implying that water being generated by the reaction is immediately adsorbed. Therefore, $q^{\star}$ can be calculated as a constant value for certain T and p, using the Langmuir-Freundlich isotherm [30]. The adsorption parameters for the shortcut model were taken from [30].

4. Case Study

To provide additional context to the limitations and the evaluation of the developed RSOC/SEDMES process, a location of Dunkirk, France is selected for the operation of an exemplary plant to be commissioned in 2030. All location based considerations such as regional regulations, sources of energy and raw materials, etc. will be based upon the selected location. The two most relevant location based boundary conditions of the RSOC/SEDMES process are the sources of renewable energy and CO_2 which are available for the production of DME. These two sources are the primary limiting factors for the production rate of DME.

4.1. CO_2 Source

Within France in the year 2021, 824 million tonnes of CO_2 were emitted, which can be divided into 7 main industrial sectors: energy production (36.1 %), metal production (16.9 %), mineral processing (15.4 %), chemical production (12.4 %), waste management (9.8 %), paper & wood processing (6.5 %), and food & beverage production (2.9 %) [57]. Of the Industrial sectors, the metal production industry has the fewest number of emission sites (≈6 %) and has the highest concentration of emissions. Therefore, the metal production industry was investigated as a supplier of CO_2. Two cities, Dunkirk and Fos-sur-Mer, are the largest CO_2 emission sites in France. 14 % of France's total CO_2 emissions (115 Mt) come from the steel production industry in these two cities [57]. In Dunkirk, to facilitate decarbonization, the construction of a DMX carbon capture facility is planned for 2025 which aims to capture 1 Mt of CO_2 per year at a molar purity of 99.7 % [58].

4.2. Renewable Energy Supply

Renewable energy production in France in 2021 is recorded as 1.195×10^8 MW, representing 24.6 % of the total national energy production [59]. Of the energy sources defined to be renewable [60], one of the two predominant sources of renewable energy is produced from wind, specifically in the north of France [59].
Off the coast of Dunkirk, an 600 MW offshore Wind farm is planned to be built in 2025 and this park has been selected as the source of renewable energy for the RSOC/SEDMES process. It is assumed that the entire production capacity is available for usage via a power purchase agreement for a price of 52.47 €/MWh [61]. The intermittent availability of wind for electricity production is considered and modelled with data from the Belgian Mermaid Wind park, a similar offshore wind farm located in the North Sea [59].

4.3. Scenarios

To evaluate the behavior and optimal operation of the RSOC/SEDMES plant, three operational scenarios based upon different electricity prices and availability are considered. For each scenario, the economic, ecologic and thermodynamic performance are calculated and evaluated.

1. **Wind park scenario:** Constant contractual electricity price with variable electricity availability of a 600 MW rated wind park.

2. **Electricity network scenario:** Fluctuating market spot price with non-limiting electricity availability from the French Electricity network.

3. **Constrained scenario:** Fluctuating market spot price with variable electricity availability of a 600 MW rated wind park.

4.4. Definition of comparison processes

To provide context to the performance of our developed process, two other DME processes were selected as reference processes.
Currently, most of the DME is produced from natural gas via the indirect reaction pathway, producing the intermediate product methanol [5]. Thus, as a state-of-the-art reference process, DME produced from natural gas is chosen.
An alternative, well-known renewable feedstock is biomass. For DME production, any lignocellulosic biomass can be used. Syngas is produced via biomass gasification, which is then converted further to DME [6]. The world's first bioDME plant is located in Sweden, using black liquor from the pulp industry as reactant [62]. However, french biomass is mostly gained from forest residue [63], so this feedstock is chosen as a second reference process (state-of-research).

5. Optimization

As a natural extension to the systematic process design, two further process optimizations are completed to determine the economically optimal operating design and operating regime for the RSOC/SEDMES plant under intermittent electricity availability and fluctuating price. A genetic algorithm (GA) [47] is used to optimize the steady state SEDMES process in a MINLP optimization, and the CPLEX solver [64] is used to solve a MILP DSM optimization problem for the RSOC process.

5.1. SEDMES: Derivative-free Optimization using a Genetic Algorithm

As opposed to heuristically selecting plant conditions and unit operation design specifications, a genetic algorithm optimization is used to complete a MINLP optimization of the SEDMES process' plant conditions and unit operation design. A genetic algorithm is a stochastic, gradient free optimization algorithm which enables the optimization of modular simulations such as Aspen Plus® process models and custom written models without requiring the rigorous calculations of derivatives [65, 66].
For this investigation, the genetic algorithm implementation from the MATLAB® global optimization toolbox is used [47] and the implementation follows the methods developed by Lee et al. [48].
All key operational variables of the SEDMES process such as number of distillation column trays, flash temperatures, purge ratios, etc. are selected and assigned an upper and lower bound determined via relevant engineering knowledge within which the genetic algorithm can iterate. The optimized variables, lower bounds, upper bounds, and optimal values be found in the supplementary
Via the Aspen Plus® MATLAB® interface, the current iteration's operational variables are set within Aspen Plus® and the resulting process model is simulated [48]. All resulting stream and unit operation results are read back into MATLAB® and the fitness of the current iteration is calculated as a net present Value (NPV) calculation as shown in Equation 9.

$$NPV = -C_I + (R - C_{OP}) \cdot (1 - t) \cdot \frac{1 - (i + i)^{-n}}{i} + D \cdot t \cdot \frac{1 - (i + i)^{-n}}{i} + \frac{C_W}{(1 + i)^n} \quad (9)$$

The NPV calculation considers the capital investment (C_I), Revenue (R), and operational costs (C_{OP}) of the plant, as well as the tax rate (t), hurdle rate (i), plant depreciation (D) and required working capital (C_W) over the plant lifetime (n) [55].
All economic calculations, such as capital investment determined via Gutherie's method and operational investments, are calculated using the methods proposed by Biegler et al. and Sieder et al. [55, 67]. A costing script was written for each unit operation in MATLAB®, which automatically sizes and costs the unit operation. Preliminary heat integration is also completed via a MATLAB® pinch based heat integration script and is considered in the capital and operational costs. Any iterations in which the Aspen Plus® process model failed to converge is considered infeasible and a significant penalty of -1×10^{20} € is added to the NPV.
The genetic algorithm has a population size of 40 individuals per generation and can iterate for a maximal of 50 generations. The crossover fraction of each generation is set to 0.4 and the optimization terminates if the fitness of the optimal individual does not change after 10 generations. The optimal SEDMES process model is determined after 14 generations and 570 iterations, requiring 102 minutes (Intel Xeon Gold 5222, 3.8 GHz, 511 GB RAM). The optimized operational variables have been described and used in Section 3.3.1.

5.2. RSOC: Dynamic Optimization with GA-built, Linearized Surrogate Models Embedded

Once the optimal parameters for the SEDMES process are determined (Section 5.1), an operating regime for the RSOC process can be designed that satisfies the continuous syngas demand of the SEDMES process.
The ability to operate the solid oxide cell in reverse mode and to store the reactants and products of the RSOC process allows the system to respond flexibly to changes in electricity price and availability. This results in a DSM optimization problem with the following degrees of freedom: For each discrete time interval in our simulation, the RSOC can either produce or consume syngas. Furthermore, the rate of production or consumption can be chosen dynamically. At each time interval, CO_2, H_2O and O_2 can be purchased externally at market prices and fed into the respective tank. In addition, excess oxygen from the tank can be sold. Syngas cannot be sold, but will only be consumed continuously by the SEDMES process and in FC phases by the RSOC process. Apart from the continuous syngas consumption of the SEDMES process and bounds on the design variables, two further constraints must be fulfilled: First, a path constraint states that at no time more energy may be used by the RSOC cell than is provided by our power source. Second, a terminal constraint states that, for each tank, the fill level at the beginning and end of the one-year simulation period must be the same. The tank size can be freely chosen by the optimizer and is reflected in the CAPEX. As an objective function, the NPV is maximized, accounting for the sale of DME and O_2 (Equation 9). For the OPEX, the sum over all time intervals is computed, whereas for the CAPEX, the maximum of all time intervals is chosen. The mathematical problem formulation is included in the supplementary materials.

For an hourly discretization, an MILP optimization problem with 236 500 equations and 210 300 variables is obtained that was solved to optimality with IBM's ILOG CPLEX V12.10 solver in GAMS V33.1 taking 450 s, 1309 s, and 60 s for each of the three scenarios respectively (Intel Xeon Gold 5222, 3.8 GHz, 511 GB RAM). It was observed that due to the staircase structure of the system, CPLEX's Barrier solver was particularly efficient in solving the problem. Furthermore, extremely careful scaling of all units and the Big-M-operator was required to overcome numerically induced infeasibilities and to obtain a well-conditioned model.

To solve this optimization problem, relationships must be given between the degrees of freedom, more precisely the rate of syngas production or consumption, and (1) the cell's electricity consumption or production, (2) the operating costs, and (3) the capital costs for the RSOC process. Since successfully representing and solving the system of thermodynamic equations underlying Aspen Plus® is hardly possible in GAMS [68], we approximate these relationships by linear surrogate models. For this purpose, we take a set of 50 equally spaced syngas production and consumption rates and employ the Genetic Algorithm (Section 5.1) to adjust the remaining RSOC process parameters so that power consumption, operating costs, and capital costs are minimized for the given flowrate.

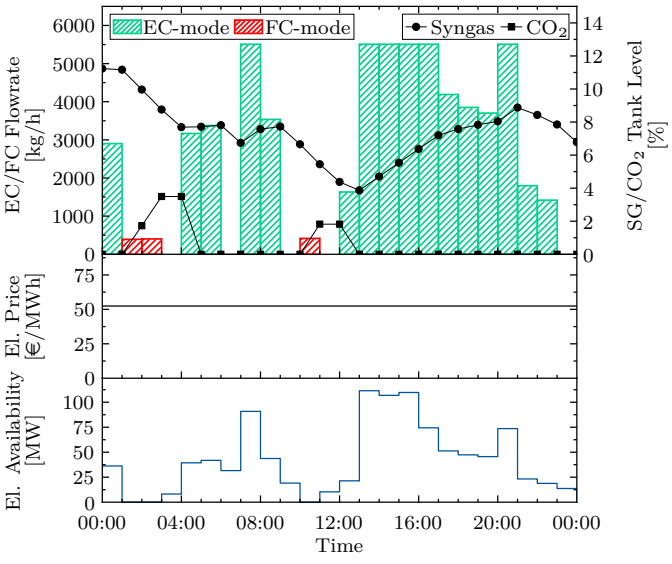

Figure 5: Optimal RSOC operating regime for the wind park scenario (variable electricity availability, constant electricity price). Data for Jan 02, 2021.

The obtained optimization results are traceable and consistent with our hypotheses. In the wind park scenario (variable electricity availability, constant electricity price), the process operates in the EC mode whenever enough electricity is available. This is sensible, since a constant electricity price offers no incentive for operation in the FC mode. To operate in the FC mode, a syngas overproduction in the EC mode is necessary and the related costs must be compensated by a higher electricity sales price in the FC phase. Such an electricity price difference does not exist in the wind park scenario. However, when the electricity availability drops to a level where the continuous electricity demand of the SEDMES process cannot be met, the RSOC has to switch to the FC mode and provide the required electricity for the SEDMES process under consumption of syngas. In summary, Figure 5 shows the optimization results for a day when the described characteristics of the first scenario are well visible.

In the electricity network scenario (non-limiting electricity availability, variable electricity price), a lower syngas production rate is sufficient since no compensation for electricity shortages is required. However, compared to a scenario with non-limiting electricity and constant prices, there still exists an overproduction of syngas for low electricity prices. This allows the process to run idle during periods with high electricity prices (Figure 6).

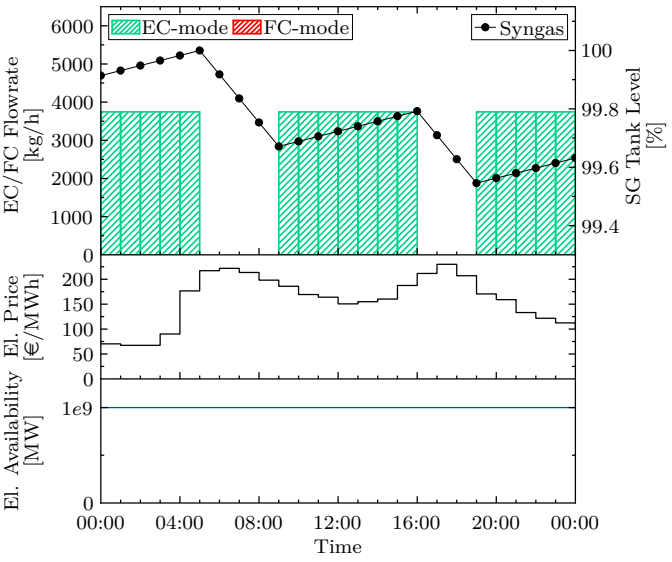

Figure 6: Optimal RSOC operating regime for the electricity network scenario (non-limited electricity availability, variable electricity price). Data for Oct 04, 2021.

There exists an equilibrium between the cost savings in these periods and the additional costs caused by the larger syngas tank. There is no operation in FC mode, since the range of electricity prices ($price_{max} - price_{min} = 686.18\,€$) is not large enough to justify the costs of further overproduction. No storage tank for CO_2 is needed.

Finally, in the constrained scenario (variable electricity availability and price), both phenomena can be observed - the increased syngas production rate of the first scenario, and the idle times of the second scenario. Remarkably, in the constrained scenario, the FC mode is not solely used for electrical self-supply during low availability periods, but also for electricity export to the grid (Figure 7). This is due to the fact that a larger syngas tank has already been built in response to the electricity shortages. Therefore, operation in the FC mode is not linked to a larger

required tank as in the electricity network scenario. The most favorable break-even price is achieved for the first scenario, as further discussed in Section 6.2.

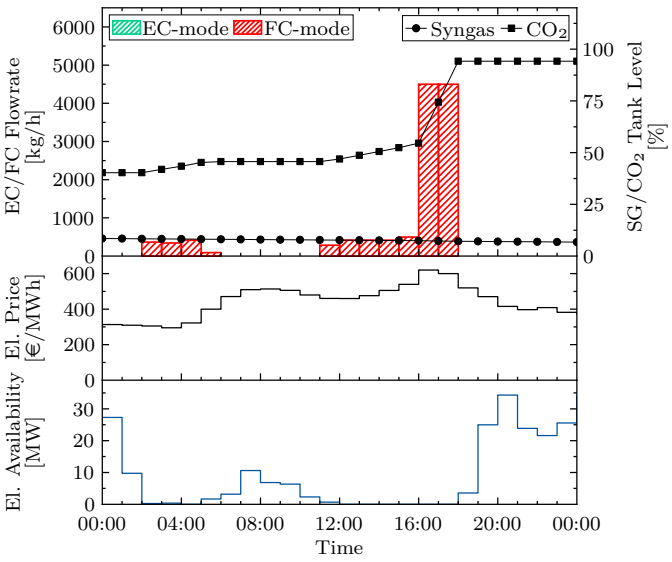

Figure 7: Optimal RSOC operating regime for the constrained scenario (variable electricity availability and price). Data for Dec 21, 2021.

When evaluating the thermodynamic, economic, and ecologic process performance in section 6, a single operating point of the plant is desired as opposed to a complex, dynamic operating regime. Therefore, we determine the average syngas production and consumption rates for each of the three scenarios. For these operating points, we then carry out the heat integration of the combined process using Aspen's Energy Analyzer and perform the final evaluation.

6. Process Performance

In the following section, the optimized process is evaluated thermodynamically, economically and ecologically for each of the three chosen scenarios and is subsequently compared to other DME synthesis pathways.

6.1. Thermodynamic Evaluation (Exergetic Efficiency)

To evaluate the thermodynamic performance of our proposed process, the exergetic efficiency is determined and compared to the exergetic efficiencies reported in literature for the reference processes of DME production [69, 70]. The exergetic efficiency η_{ex} is defined as the ratio of the total amount of useful exergy leaving the system (E_{out}) [69], i.e. the exergetic sum of the DME, O_2 and produced electricity streams, to the total amount of exergy entering the system (E_{in}) [71].

$$\eta_{ex} = \frac{E_{out}}{E_{in}} \tag{10}$$

Electricity is classified as pure exergy. After plant wide heat integration, the remaining required heating is provided via electric heaters, which consequently consume pure exergy. The exergy of a material stream is composed of the physical and chemical exergy [71]. The calculations and exergies of all streams are listed in the supplementary material. The exergetic efficiencies of the three investigated scenarios are depicted in Figure 8. Our process reaches an exergetic efficiency of 49.2 %, 53.2 % and 49.4 % in the scenarios 1,2 and 3, respectively. Bin et al. investigated the exergy streams of the state-of-the-art, natural gas to DME [70]. Based on their data an exergietic efficiency of 37.7 % is calculated. Thus, in every scenario, our process outperforms the natural gas based reference case. For the second reference process, biomass to DME, Parvez et al. estimate an efficiency of about 50.8 % [69]. This is slightly better than the thermodynamic performance of the RSOC/SEDMES process in scenario 1 and 3. However, in scenario 2 our process exceeds the efficiencies of both reference cases. In this case, no electricity is generated in the FC mode. The cell operates only in the EC mode and thus avoids exergy destruction. The exergies of the material streams do not vary significantly between the three scenarios.

The high exergetic efficiency of the proposed process is, in part, due to the plant wide heat integration which utilizes the high energy levels of the RSOC to completely fulfill the remaining heating requirements of the RSOC and SEDMES processes.Furthermore, heat integration reduce the amount of required external cooling by over 70 %. This emphasizes the potential and necessity of integrating processes, as the large amount of waste heat generated by the RSOC would otherwise be lost and result in an abysmal exergetic efficiency.

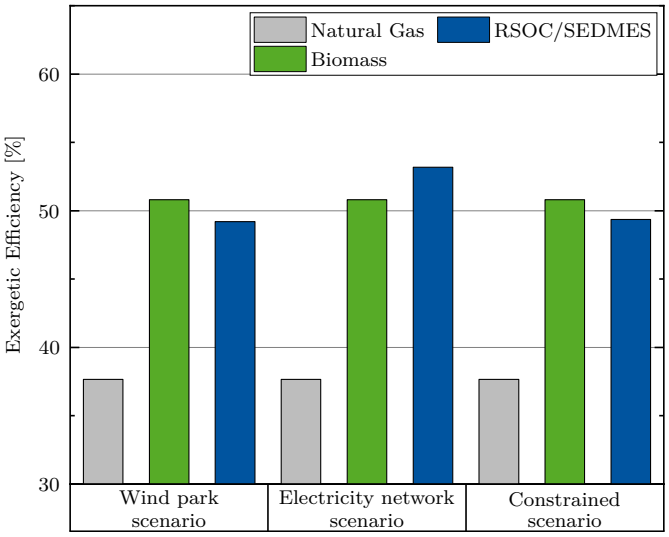

Figure 8: Thermodynamic process performance

6.2. Economic Evaluation

The economic performance of the RSOC/SEDMES process in each of the three scenarios is evaluated via the NPV and DME break-even price. The NPV of the combined process is calculated in GAMS as described in Section 5.2 with Equation 9.

The capital cost calculations completed in Section 5.1 use Gutherie's method and assume an update factor of 591.1 [72]. The operating costs are calculated to include the costs of labor, raw materials, waste disposal, yearly tax, maintenance, electricity, heating, and cooling. The working capital is calculated to include additional capital for one month of accounts receivable, accounts payable, operational costs, and raw material inventory [55, 67]. The tax rate, hurdle rate, and plant lifetime are assumed to be 3%, 10% and 25 years respectively. Plant depreciation is modeled via linear depreciation.

At a current market price of 0.40 €/kg DME [73], all three investigated scenarios are non-profitable. The wind park scenario is the most profitable of the investigated scenarios with an NPV of -318×10^6 € and a break-even price of 2.14 €/kg_{DME}. The electricity network and constrained scenarios have a NPV and break-even price of -331×10^6 €, 2.21 €/kg_{DME} and -400×10^6 €, 2.59 €/kg_{DME} respectively.

In the wind park scenario, due to the reversible nature of the RSOC/SEDMES process, we are able to take advantage of the very low renewable electricity prices via a power purchase agreement without being limited by the influence of intermittent electricty availibility on the production of the steady state SEDMES process. The potential of such flexible processes to have a low ecological impact and be more economically feasible than using electricity from the fossil based electricity grid shows great promise for transitioning the chemical industry to renewable energy sources.

Comparing the RSOC/SEDMES process with the state of the art and state of research processes, as well a further, similar conventional CO_2 to DME process [74], our developed process shows encouraging results. Of the renewable processes currently being researched for green production of DME, our RSOC/SEDMES has the lowest break-even price. The state of research process has a break-even price of 2.64 €/kg) [75] and the similar CO_2 to DME process reported by Pacheco et al. has a break price of 6.43 €/kg) [74]. However, the developed RSOC/SEDMES process can not compare to the state-of-the-art production method which sells DME at the current market price of 0.40 €/kg_{DME} [73].

A sensitivity analysis of the NPV is also completed for two predominant economic factors: the tax rate and the hurdle rate. As the behavior of all three scenarios are similar for this sensitivity analysis, only the sensitivity of the wind park scenario (scenario 1) will be depicted.

The NPV does not show a strong sensitivity to the hurdle rate. The NPV cannot become economically neutral for any hurdle rate. For a hurdle rate of 0 % the NPV remains negative with a value of -310×10^6 €. Decreasing the tax rate from 3 % to 0 % only has a trivially small effect on the NPV.

6.3. Ecological Evaluation (Life Cycle Assessment)

The ecological impact of the RSOC/SEDMES process is evaluated in comparison to two other DME production processes (cf. Section 4.4) by analyzing the greenhouse gas emissions (GHG). As GHGs we consider CO_2 (including CO and VOC) and the CO_2 equivalents of CH_4 and N_2O. This assessment of the processes' utilization of captured carbon dioxide is based on the Greenhouse gases, Regulated Emissions, and Energy use in Transportation (GREET®) model developed at the Argonne National Laboratory (ANL) [76]. The LCA analysis of the RSOC/SEDMES process and all reference processes utilize a cradle-to-gate system boundary. As all processes produce DME, the gate-to-grave emissions are equivalent for all processes. The functional unit is 1 kg of DME. As the RSOC/SEDMES process produces oxygen and electricity as byproducts which exit the system boundaries, the reference processes must also account for additional oxygen and electricity production to remain comparable. This is done via a system expansion which means that the GHG emission caused by the production of the byproducts are added to DME production and not attributed to oxygen or electricity as a product.

Wastewater treatment, construction and recycling/disposal of the plant as well as of catalysts and adsorbent are not accounted for in the LCA, as it neither has been for the reference processes in GREET®. The considered streams are depicted in Figure 9. In scenarios 1 and 3 the electricity input is provided by wind energy, whereas scenario 2 uses the electricity mix of the French electricity network. The complete Life cycle inventory, including detailed information about the composition of GHGs, is provided in the supplementary material.

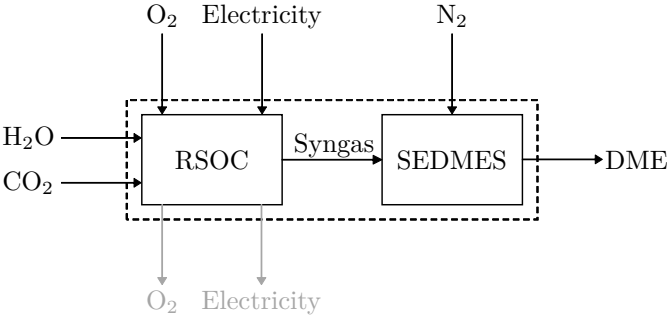

Figure 9: Streams considered in the Life Cycle Inventory.

Also, transportation is neglected except from the non-local natural gas as reactant in the state-of-the-art reference process. It is considered to be transported by pipelines from Norway, which is the nearest country with greater

natural gas resources and exports [77]. A straight pipeline transportation is estimated, with a distance of (606 km from Troll gas field in the norwegian north sea to Dunkirk. The consumed electricity mix of the reference processes is modeled by the current electricity mix in France: residual oil: 0.32 %, natural gas: 6.16 %, coal: 0.78 %, nuclear: 68.18 %, biomass: 0.93 %, others: 23.63 % [59]. The LCA is performed in the first year of operation which is assumed to be 2030. For the state-of-the-art process, the production capacity of a small scale DME plant is selected (25 MT/day) which is close to the production capacity of the developed process [5].

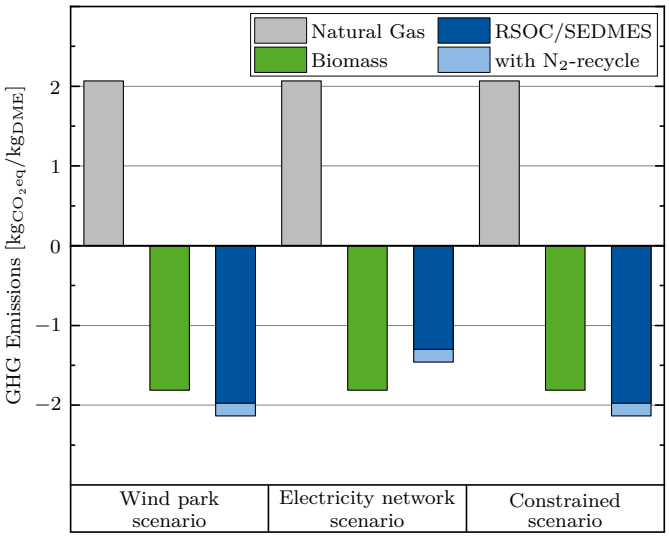

Figure 10: Ecological Process Performance.

Figure 10 depicts the GHG emissions of our process and the two reference processes for the three scenarios described in Section 4.3. The light blue parts depict additional GHG savings, if 80 % of the nitrogen required for desorption is recycled, despite being economically infeasible (cf. Section 3.3.2). The results of the LCA does not meaningfully vary between scenarios 1 and 3 (about $-1.97\,\mathrm{kg_{CO_2eq}/kg_{DME}}$). In scenario 2, the potential GHG reduction decreases to $-1.3\,\mathrm{kg_{CO_2eq}/kg_{DME}}$ because the electricity supplied by the grid instead of renewable wind energy causes increased emissions during electricity generation. Recycling of nitrogen would cause additional GHG savings of about $-0.16\,\mathrm{kg_{CO_2eq}/kg_{DME}}$. The ecological performance of the RSOC/SEDMES process remains in all scenarios superior to the state-of-the-art process (about $2.07\,\mathrm{kg_{CO_2eq}/kg_{DME}}$). The GHG emissions of the reference processes do not vary significantly between the three cases. Compared to the state-of-research process (about $-1.81\,\mathrm{kg_{CO_2eq}/kg_{DME}}$), the RSOC/SEDMES process only has a better ecological impact in scenarios 1 and 3, when electricity is provided from renewable sources. This suggests that the implementation of the proposed process only outperforms the state-of-research process, if the electricity for our proposed process is provided by renewable sources. Furthermore, these results reaffirm the key role that emissions connected to electricity generation play in the overall ecological performance of the proposed process. This emphasizes the importance of incorporating renewable energy sources into the development of innovative processes, in order to maximize the CO_2 mitigation potential. It needs to be kept in mind, that LCA on the presented scope is a tool for comparison of process alternatives between each other in terms of ecological performance. Therefore, it is not possible to conclude from the negative GHG emissions, if the entire RSOC/SEDMES process is a net negative or net positive GHG emitter. What can be concluded however is that the developed RSOC/SEDMES process represents a significant improvement over other currently implemented DME processes.

7. Conclusion

This work presents a novel chemical process for the conversion of captured carbon dioxide to dimethyl ether using intermittently available renewable energy sources. After evaluating many viable chemical products and production pathways via a semi quantitative systematic screening, a promising combined reversible solid oxide cell and sorption enhanced DME synthesis process is selected and designed. The process models are modelled within Aspen Plus® while also employing custom models written in MATLAB® for nonexistent unit operations. A process optimization (MINLP) and demand side management (MILP) optimization problem, solved via a genetic algorithm and the CPLEX solver respectively, are formulated within MATLAB® and GAMS to determine the optimal operating design and production regime of the developed process.

Three different production scenarios with varying electricity prices and availabilities are investigated and the results of each scenario are compared with a state-of-the-art (natural gas based) and a state-of-research (biomass based) process to determine the contextualized performance of the developed process.

The ecological impact of the process is calculated via a cradle-to-gate life cycle analysis using data collected from the GREET® database. The developed process has a GHG emission of $-1.973/-1.299/-1.973\,\mathrm{kg_{CO_2\ eq}/kg_{DME}}$ (scenario 1/2/3) which represents a massive improvement over the state-of-the-art process in all scenarios and a slight improvement over the state-of-research process in most scenarios. The economic viability of the process is calculated via a net present value calculation determined within the demand side management optimization in GAMS. The net present value considers the primary capital & operational investments, including factors such as depreciation and necessary working capital. Via a sensitivity analysis, the break even price of DME for each scenario is calculated, $2.14/2.21/2.59\,€/\mathrm{kg_{DME}}$ (scenario 1/2/3). For current market prices of DME set by the state-of-the-art process, the combined RSOC/SEDMES process is not economically

viable and requires at least a 5.35 factor price multiplication to become viable. However, amongst the alternative non-fossil based DME processes, the RSOC/SEDMES process is the most economically viable. After completing plantwide heat integration, the thermodynamic performance of the process is calculated and represented via the exergetic efficiency. The developed process has an exergetic efficiency of 49.2 %/53.2 %/49.4 % and is therefore more efficient than the state-of-the-art process and is similar to the state-of-research process.

This paper concludes that the developed RSOC/SEDMES process represents a very promising design to efficiently produce DME from captured CO_2 and renewable energy sources. The ecologic, economic and thermodynamic results of the process are comparable or superior to those of similar processes. It is the opinion of the authors, that with continuing technological development, this proposal represents a viable option as a renewable and sustainable process for the future.

Supplementary Information is attached.

References

[1] United Nations. *Paris Agreement* `https://unfccc.int/sites/default/files/english_paris_agreement.pdf` (2022).

[2] Kätelhön, A. *et al.* Climate change mitigation potential of carbon capture and utilization in the chemical industry. eng. *Proceedings of the National Academy of Sciences of the United States of America* **116,** 11187–11194 (2019).

[3] Wang, L. *et al.* Reversible solid-oxide cell stack based power-to-x-to-power systems: Comparison of thermodynamic performance. *Applied Energy* **275,** 115330 (2020).

[4] van Kampen, J. *et al.* Sorption enhanced dimethyl ether synthesis for high efficiency carbon conversion: Modelling and cycle design. *Journal of CO2 Utilization* **37,** 295–308 (2020).

[5] Lee, U. *et al.* Well-to-Wheels Emissions of Greenhouse Gases and Air Pollutants of Dimethyl Ether from Natural Gas and Renewable Feedstocks in Comparison with Petroleum Gasoline and Diesel in the United States and Europe. *SAE International Journal of Fuels and Lubricants* **9,** 546–557 (2016).

[6] Lecksiwilai, N. *et al.* Net Energy Ratio and Life cycle greenhouse gases (GHG) assessment of bio-dimethyl ether (DME) produced from various agricultural residues in Thailand. *Journal of Cleaner Production,* 523–531 (2016).

[7] Chauvy, R. *et al.* Selecting emerging CO2 utilization products for short- to mid-term deployment. *Applied Energy* **236,** 662–680 (2019).

[8] Zimmermann, A. W. *et al.* Techno-Economic Assessment Guidelines for CO2 Utilization. *Frontiers in Energy Research* **8,** 5 (2020).

[9] Roh, K. *et al.* Early-stage evaluation of emerging CO2 utilization technologies at low technology readiness levels. *Green Chem.* **22,** 3842–3859 (12 2020).

[10] Artz, J. *et al.* Sustainable Conversion of Carbon Dioxide: An Integrated Review of Catalysis and Life Cycle Assessment. *Chemical Reviews* **118,** 434–504 (2018).

[11] Afzal, S. *et al.* in *27th European Symposium on Computer Aided Process Engineering* 2617–2622 (Elsevier, 2017).

[12] Catizzone, E. *et al.* CO_2 Recycling to Dimethyl Ether: State-of-the-Art and Perspectives. *Molecules (Basel, Switzerland)* **23** (2017).

[13] Graves, C. *et al.* Co-electrolysis of CO2 and H2O in solid oxide cells: Performance and durability. *Solid State Ionics* **192,** 398–403 (2011).

[14] Guffanti, S. *et al.* Reactor modelling and design for sorption enhanced dimethyl ether synthesis. *Chemical Engineering Journal* **404,** 126573 (2021).

[15] Rezaei, E. *et al.* Techno-economic comparison of reverse water gas shift reaction to steam and dry methane reforming reactions for syngas production. *Chemical Engineering Research and Design* **144,** 354–369 (2019).

[16] Serrano-Lotina, A. *et al.* Influence of the operating parameters over dry reforming of methane to syngas. *International Journal of Hydrogen Energy* **39,** 4089–4094 (2014).

[17] Wang, Y. *et al.* High temperature solid oxide H2O/CO2 co-electrolysis for syngas production. *Fuel Processing Technology* **161,** 248–258 (2017).

[18] Jens, C. M. *et al.* Rh-Catalyzed Hydrogenation of CO 2 to Formic Acid in DMSO-based Reaction Media: Solved and Unsolved Challenges for Process Development. *Advanced Synthesis & Catalysis* **361,** 307–316 (2019).

[19] Pérez-Fortes, M. *et al.* Formic acid synthesis using CO2 as raw material: Techno-economic and environmental evaluation and market potential. *International Journal of Hydrogen Energy* **41,** 16444–16462 (2016).

[20] Pérez-Fortes, M. *et al.* Methanol synthesis using captured CO2 as raw material: Techno-economic and environmental assessment. *Applied Energy* **161,** 718–732 (2016).

[21] Joo, O.-S. *et al.* Carbon Dioxide Hydrogenation To Form Methanol via a Reverse-Water-Gas-Shift Reaction (the CAMERE Process). *Industrial & Engineering Chemistry Research* **38,** 1808–1812 (1999).

[22] Al-Kalbani, H. *et al.* Comparative energetic assessment of methanol production from CO2: Chemical versus electrochemical process. *Applied Energy* **165,** 1–13 (2016).

[23] Kim, J. *et al.* Methanol production from CO2 using solar-thermal energy: process development and techno-economic analysis. *Energy & Environmental Science* **4,** 3122 (2011).

[24] Sánchez, A. *et al.* Sustainable DMC production from CO2 and renewable ammonia and methanol. *Journal of CO2 Utilization* **33,** 521–531 (2019).

[25] Garcia-Herrero, I. *et al.* Environmental Assessment of Dimethyl Carbonate Production: Comparison of a Novel Electrosynthesis Route Utilizing CO 2 with a Commercial Oxidative Carbonylation Process. *ACS Sustainable Chemistry & Engineering* **4,** 2088–2097 (2016).

[26] Fernández-Dacosta, C. *et al.* Prospective techno-economic and environmental assessment of carbon capture at a refinery and CO2 utilisation in polyol synthesis. *Journal of CO2 Utilization* **21,** 405–422 (2017).

[27] Müller, B. *et al.* Energiespeicherung mittels Methan und energieetragenden Stoffen - ein thermodynamischer Vergleich. *Chemie Ingenieur Technik* **83,** 2002–2013 (2011).

[28] van der Giesen, C. *et al.* Energy and climate impacts of producing synthetic hydrocarbon fuels from CO(2). *Environmental science & technology* **48,** 7111–7121 (2014).

[29] Schakel, W. *et al.* Assessing the techno-environmental performance of CO2 utilization via dry reforming of methane for the production of dimethyl ether. *Journal of CO2 Utilization* **16,** 138–149 (2016).

[30] van Kampen, J. *et al.* Separation enhanced methanol and dimethyl ether synthesis. *Journal of Materials Chemistry A* **9,** 14627–14629 (2021).

[31] Li, H. *et al.* The high-yield direct synthesis of dimethyl ether from CO 2 and H 2 in a dry reaction environment. *Journal of Materials Chemistry A* **9,** 2678–2682 (2021).

[32] Botta, G. *et al.* Thermodynamic Analysis of Coupling a SOEC in Co-Electrolysis Mode with the Dimethyl Ether Synthesis. *Fuel Cells* **15,** 669–681 (2015).

[33] Pozzo, M. *et al.* Enhanced biomass-to-liquid (BTL) conversion process through high temperature co-electrolysis in a solid oxide electrolysis cell (SOEC). *Fuel* **145,** 39–49 (2015).

[34] Skorikova, G. *et al.* The Techno-Economic Benefit of Sorption Enhancement: Evaluation of Sorption-Enhanced Dimethyl Ether Synthesis for CO2 Utilization. *Frontiers in Chemical Engineering* **2** (2020).

[35] Santhanam, S. *Process systems analysis of reversible Solid Oxide Cell (rSOC) reactors for electricity storage and sector coupling* Institute of Energy Storage (University of Stuttgart, Stuttgart, 2018). 292 pp.

[36] Venkataraman, V. *et al.* Reversible solid oxide systems for energy and chemical applications – Review & perspectives. *Journal of Energy Storage* **24,** 100782 (2019).

[37] Er-rbib, H. *et al.* Performance assessment of a power-to-gas process based on reversible solid oxide cell. *Frontiers of Chemical Science and Engineering* **12,** 697–707 (2018).

[38] Azizi, Z. *et al.* Dimethyl ether: A review of technologies and production challenges. *Chemical Engineering and Processing: Process Intensification* **82,** 150–172 (2014).

[39] Hauck, M. *et al.* Simulation of a reversible SOFC with Aspen Plus. *International Journal of Hydrogen Energy* **42,** 10329–10340 (2017).

[40] Kazempoor, P. *et al.* Model validation and performance analysis of regenerative solid oxide cells for energy storage applications: Reversible operation. *International Journal of Hydrogen Energy* **39,** 5955–5971 (2014).

[41] Schmidt, V. M. *Elektrochemische Verfahrenstechnik. Grundlagen, Reaktionstechnik, Prozeßoptimierung* 660 pp. (Wiley, Weinheim, 2003).

[42] Bustamante, F. *et al.* High-temperature kinetics of the homogeneous reverse water-gas shift reaction. *AIChE Journal* **50,** 1028–1041 (2004).

[43] Redissi, Y. *et al. Storage and restoring the electricity of renewable energies by coupling with natural gas grid* in *The International Renewable and Sustainable Energy Conference (IRSEC'13)* (ISBN 978-1-4673-6374-7/13, Ouarzazate, Morocco, Mar. 2013), pp. 430–435. https://hal-mines-paristech.archives-ouvertes.fr/hal-01463695.

[44] Konrad Motylinski *et al.* Dynamic modelling of reversible solid oxide cells for grid stabilization applications. *Energy Conversion and Management* **228,** 113674. https://www.sciencedirect.com/science/article/pii/S0196890420312000 (2021).

[45] Francesco Lonis *et al.* Assessment of integrated energy systems for the production and use of renewable methanol by water electrolysis and CO2 hydrogenation. *Fuel* **285,** 119160. https://www.sciencedirect.com/science/article/pii/S0016236120321566 (2021).

[46] Aspen Technology, I. Physical Property Methods and Models 11.1.

[47] *MATLAB Optimization Toolbox* The MathWorks, Natick, MA, USA. 2019.

[48] Lee, U. *et al.* Techno-economic Optimization of a Green-Field Post-Combustion CO 2 Capture Process Using Superstructure and Rate-Based Models. *Industrial & Engineering Chemistry Research* **55,** 12014–12026 (2016).

[49] Bard, A. J. *et al. Electrochemical Methods. Fundamentals and Applications* 2nd Edition. 850 pp. (John Wiley & Sons Inc., New York, 2001).

[50] Bove, R. *et al. Modeling solid oxide fuel cells. Methods, procedures and techniques* xiv, 395 (Springer, Berlin, 2008).

[51] (ed Merck KGaA) *Dimethylether* https://www.sigmaaldrich.com/DE/de/substance/dimethylether4607115106 (2022).

[52] ISO/IEC, 2010. ISO 16861:2015(E). *Petroleum products - Fuels (class F) - Specifications of dimethyl ether (DME)*

[53] Brunetti, A. *et al.* Membrane technologies for CO2 separation. *Journal of Membrane Science* **359,** 115–125 (2010).

[54] *Power to Fuel: 6 - Power-to-DME: a cornerstone towards a sustainable energy system* (eds Semmel, M. *et al.*) (Elsevier, 2021).

[55] Biegler, L. *et al. Systematic Methods of Chemical Process Design* (Prentice Hall PTR, 1997).

[56] Styles, C. Costs of nitrogen gas – how much should you be paying? *Purity Gas Inc.* https://puritygas.ca/nitrogen-gas-costs/ (2022) (2017).

[57] Agency, E. E. *Industrial Reporting under the Industrial Emissions Directive 2010/75/EU and European Pollutant Release and Transfer Register Regulation (EC) No 166/2006* 2021. https://www.eea.europa.eu/data-and-maps/data/industrial-reporting-under-the-industrial-4.

[58] Dunkirk, D. D. *3D Project* 2022. https://3d-ccus.com/3d-overview/.

[59] (ed ENTSO-E) *Transparency Platform* https://transparency.entsoe.eu (2022).

[60] francaise, R. *Code de l'energie, Article L211-2* 2021. https://www.legifrance.gouv.fr/codes/article_lc/LEGIARTI000043213358.

[61] Energy, L. *Q4 2021 PPA Price Index* 2021. https://www.leveltenenergy.com/post/q4-2021.

[62] Fleisch, T. H. *et al.* Introduction and advancement of a new clean global fuel: The status of DME developments in China and beyond. *Journal of Natural Gas Science and Engineering* **9,** 94–107 (2012).

[63] edf. *Qu'est-ce que la biomasse ? L'énergie issue de la biomasse est une source d'énergie renouvelable qui dépend du cycle de la matière vivante végétale et animale.* 2022. https://www.edf.fr/.

[64] Cplex, I. I. V12. 1: User's Manual for CPLEX. *International Business Machines Corporation* **46,** 157 (2009).

[65] Holland, J. H. *Adaptation in Natural and Artificial Systems: An Introductory Analysis with Applications to Biology, Control and Artificial Intelligence* (MIT Press, Cambridge, MA, USA, 1992).

[66] Leboreiro, J. *et al.* Processes synthesis and design of distillation sequences using modular simulators: a genetic algorithm framework. *Computers & Chemical Engineering* **28,** 1223–1236 (2004).

[67] Seider, W. D. *et al. Product and Process Design Principles: Synthesis, Analysis and Evaluation, 4th Edition* (Wiley, 2004).

[68] Goldstein, D. *et al.* Multilevel surrogate modeling of an amine scrubbing process for CO2 capture. *AIChE Journal (In Production)* (2022).

[69] Parvez, A. M. *et al.* Bio-DME production based on conventional and CO 2 -enhanced gasification of biomass: A comparative study on exergy and environmental impacts. *Biomass and Bioenergy* **110,** 105–113 (2018).

[70] Bin, C. *et al.* System study on natural gas-based polygeneration system of DME and electricity. *International Journal of Energy Research* **32,** 722–734 (2008).

[71] Xiang, Y. *et al.* Exergetic evaluation of renewable light olefins production from biomass via synthetic methanol. *Applied Energy* **157,** 499–507 (2015).

[72] Access Intelligence. *Chemical Engineering: Economic Indicator* https://ic.nipc.ir/ic/Portals/0/Introduce/cost%5C%20index/Chemical%5C%20Engineering%5C%20Vol127%5C%239%5C%20Sep2020.pdf (2022).

[73] Wu, T.-W. *et al.* A novel energy-efficient process of converting CO2 to dimethyl ether with techno-economic and environmental evaluation. *Chemical Engineering Research and Design* **177,** 1–12 (2022).

[74] Pacheco, K. A. *et al.* Multi criteria decision analysis for screening carbon dioxide conversion products. *Journal of CO2 Utilization* **43,** 101391. https://www.sciencedirect.com/science/article/pii/S2212982020310210 (2021).

[75] Baena-Moreno, F. M. *et al.* Exploring profitability of bioeconomy paths: Dimethyl ether from biogas as case study. *Energy* **225,** 120230. https://www.sciencedirect.com/science/article/pii/S0360544221004795 (2021).

[76] Argonne National Laboratory. *GREET®: Greenhouse gases, Regulated Emissions, and Energy use in Transportation* 2021. https://greet.es.anl.gov/greet_excel_model.models (2022).

[77] CIA. *Field Listing - Natural gas – production* The world factbook, 2022. https://www.cia.gov/the-world-factbook/field/natural-gas-production/.